PHILOSOPHICAL TRANSACTIONS OF THE ROYAL SOCIETY A MATHEMATICAL, PHYSICAL & ENGINEERING SCIENCES

Unimolecular Dissociation: An Eigenchannel Generalized Quantum View [and Discussion]

M. S. Child, J. C. Light and N. C. Handy

Phil. Trans. R. Soc. Lond. A 1990 **332**, 273-282
doi: 10.1098/rsta.1990.0114

Unimolecular dissociation: an eigenchannel generalized quantum view

By M. S. Child

Theoretical Chemistry Department, University of Oxford, 5 South Parks Road, Oxford OX1 3UB, U.K.

A quantum mechanical eigenchannel theory of unimolecular dissociation is outlined with specific reference to systems with many closed and few open channels. The resonances (whose lifetimes determine state specific dissociation rates) are shown to decay at rates determined by the fractional open channel weightings in the relevant eigenchannels, while the relative weightings between the open channels determines the fragment internal state distribution. An isolated resonance, random eigenvector version of the theory bears a similarity with established statistical theories. A simplified model application to the in plane dissociation of HCN is reported, for which 60 channels are required for convergence. The decay rates for different resonances are found to be broadly statistical, but the fragment state distributions vary markedly from one resonance to another even when dynamical interactions between many overlapping resonances are taken into account.

1. Introduction

The conventional RRKM theory of unimolecular decomposition (Robinson & Holbrook 1972; Forst 1973) separates the molecular space into internal and external parts separated by the transition state, in such a way that the decomposition rate appears as a ratio of the state density at the transition state to that in the internal region. This paper seeks to analyse the nature of these 'states' from a consistent quantum mechanical viewpoint that encompasses both bound and decomposing states, with the object of providing a framework for interpretation of the new generation of state specific experiments (Guyer *et al.* 1984; Carrington & Kennedy 1984; Reisler & Wittig 1986; Butler *et al.* 1986). The questions raised concern the statistical or non-statistical character of individual decay rates and the factors that affect the observed distribution of the fragments over their possible internal states.

The theory is presented from an internal collision (Waite & Miller 1980, 1981; Holmer & Child 1983) or generalized quantum defect (Mies & Julienne 1984) viewpoint, which draws on the elaborate structure of multichannel quantum defect theory (Seaton 1983; Greene & Jungen 1985) by modifying the boundary conditions to handle other than coulombic long-range interactions. The essential feature is to visualize the internal motions as a sequence of internal collisions between the ultimate fragments of which perhaps only a small fraction lead to escape. Consequently the theory revolves around a large internal scattering matrix whose order depends on the total number of interacting channels; the aim is to relate this matrix to the much smaller physical S matrix relevant to scattering between the channels that are open to escape. Several lines of development may be followed but Fano's (1970) eigenchannel approach proves particularly convenient because these

Phil. Trans. R. Soc. Lond. A (1990) **332**, 273–282 *Printed in Great Britain*

eigenchannels (of the internal S matrix) are found to support the 'states' observed in any time independent experiment; they correspond to the true bound states if all channels are closed and go over naturally to resonant or scattering states as more and more channels open up. Moreover, each such eigenchannel typically has weightings in all channels such that the fractional open channel weighting controls the decay rate of the resonance and the relative open channel components determine the resultant fragment state populations. Special simplicities apply if the individual resonances are assumed to decay independently, but inter-resonance interactions are also readily taken into account.

The overall structure of the theory, which employs the boundary conditions of Holmer & Child (1983) within the Fano (1970) eigenchannel description, is outlined in §2. Section 3 analyses the isolated resonance approximation with particular reference to the 'statistical' or 'non-statistical' nature of the dynamics. Section 4 then contains an illustrative application to a simplified model for dissociation of the HCN molecule, in which the internal S matrix is obtained within the sudden approximation. Finally, the main results and conclusions are summarized in §5.

2. The eigenchannel picture

The elements of the theory are illustrated in figure 1, in which the box labelled Σ represents a short-range large $N\times N$ internal-scattering matrix, which is assumed to take into account all interchannel coupling. N is therefore the number of channels that are classically open at the boundary R_c of the interaction region. Beyond R_c many of the channels will close, as depicted by the loops in figure 1, and this closing imposes constraints on the relative phases of incoming and outgoing motion at the outer turning points. The first step in the argument is to express the physical scattering matrix S between the n open channels in terms of the elements of the large matrix Σ, by taking the above phase constraints into account.

It is convenient to follow Holmer & Child (1983) in defining Σ by means of the equations

$$\psi_j^{(i)} \overset{R>R_c}{\approx} k_j^{-\frac{1}{2}}(R)\,[\delta_{ij}\,\mathrm{e}^{-\mathrm{i}\phi_j(R)} - \Sigma_{ij}\,\mathrm{e}^{\mathrm{i}\phi_j(R)}], \tag{1}$$

where

$$\phi_j(R) = \int_{a_j}^{R} k_j(R)\,\mathrm{d}R + \tfrac{1}{4}\pi,$$

$$k_j(R) = \{2m[E - V_j(R)]\}^{\frac{1}{2}}/\hbar, \tag{2}$$

and a_j is the inner classical turning point in the jth channel. Note that Mies & Julienne (1984) adopt an R dependent equivalent to the matrix Σ, but that the Σ adopted here is taken as a constant on the grounds that significant interactions are assumed to be restricted to the region $R < R_c$. Secondly, the $V_j(R)$ appearing in equation (2) are convenient mean potentials averaged over the internal motions of the system; their choice is arbitrary provided they converge to proper limits as $R\to\infty$ because different choices lead to different phases for the Σ_{ij}, which are compensated by different phase terms $\phi_j(R)$.

The next step is to re-express equation (1) in the equivalent form

$$\psi_j^{(i)} \overset{R>R_c}{\approx} k_j^{-\frac{1}{2}}(R)\,\mathrm{e}^{-\mathrm{i}(\alpha_i-\frac{1}{2}\pi)}[\delta_{ij}\,\mathrm{e}^{-\mathrm{i}\bar{\phi}_j(R)} + \tilde{\Sigma}_{ij}\,\mathrm{e}^{\mathrm{i}\bar{\phi}_j(R)}], \tag{3}$$

where

$$\bar{\phi}_j(R) = \int_{b_j}^{R} k_j(R)\,\mathrm{d}R - \tfrac{1}{4}\pi = \phi_j(R) - \alpha_j - \tfrac{1}{2}\pi, \tag{4}$$

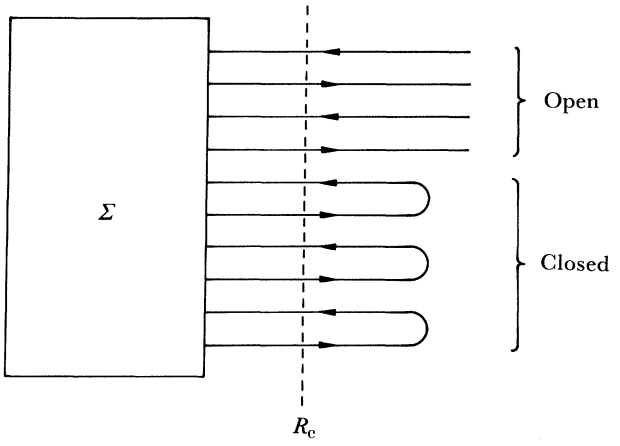

Figure 1. Diagrammatic representation of the elements of the theory.

$$\alpha_j = \int_{a_j}^{b_j} k_j(R)\,\mathrm{d}R, \tag{5}$$

and

$$\tilde{\Sigma}_{ij} = \mathrm{e}^{\mathrm{i}\alpha_i}\Sigma_{ij}\,\mathrm{e}^{\mathrm{i}\alpha_j}. \tag{6}$$

The quantities b_j are the outer classical turning points for the closed channels or the coordinate of the transition state (normally identified as an adiabatic barrier maximum) for the open channels. Note that the $V_j(R)$ in equation (2) are assumed to include centrifugal terms, and that barrier penetration corrections that are currently neglected may be included along the lines of a recent paper by Child (1986).

The elimination of closed channels proceeds by assuming the following eigenphase representation for the large, phase modified, matrix $\tilde{\Sigma}$ (Fano 1970; Aquilanti & Cavalli 1987):

$$\tilde{\Sigma}_{ij} = \sum_k \tilde{T}_{ik}\,\mathrm{e}^{2\mathrm{i}\delta_k}T_{kj}, \tag{7}$$

where T is a real orthogonal matrix and $\tilde{T}$ is its transpose. Any symmetric unitary matrix $\tilde{\Sigma}$ may be factored in this form. It follows on substitution in equation (3) that

$$\psi_j^{(i)} \overset{R>R_c}{\approx} k_j^{-\frac{1}{2}}(R)\,\mathrm{e}^{-\mathrm{i}\alpha_i-\mathrm{i}\pi/2}\sum_k \tilde{T}_{ik}[\mathrm{e}^{-\mathrm{i}\bar{\phi}_j}+\mathrm{e}^{2\mathrm{i}\delta_k}\,\mathrm{e}^{\mathrm{i}\bar{\phi}_j}]\,T_{kj}, \tag{8}$$

from which the sum over k may be eliminated by means of the transformation

$$\begin{aligned}\psi_j^{(l)} &= \sum_i T_{li}\,\psi_j^{(i)}\,\mathrm{e}^{\mathrm{i}(\alpha_i+\frac{1}{2}\pi)}\\ &\overset{R>R_c}{\approx} k_j^{-\frac{1}{2}}(R)\,[(1+\mathrm{e}^{2\mathrm{i}\delta_l})\cos\bar{\phi}_j(R)-\mathrm{i}(1-\mathrm{e}^{2\mathrm{i}\delta_l})\sin\bar{\phi}_j(R)]\,T_{lj}.\end{aligned} \tag{9}$$

Equation (9) defines the eigenchannel representation. The next step is to form n combinations of these new function vectors $\psi^{(l)}(R)$,

$$\psi^{(\alpha)}(R) = \sum_l B_{\alpha l}\,\psi^{(l)}(r), \quad \alpha = 1, 2, \ldots, n \tag{10}$$

and to require that

$$\psi_j^{(\alpha)}(R) = k_j^{-\frac{1}{2}}(R)\left[\delta_{\alpha j}\sin\left(\int_{b_j}^{R} k_j(R)\,\mathrm{d}R+\tfrac{1}{4}\pi\right)+K_{\alpha j}\cos\left(\int_{b_j}^{R} k_j(R)\,\mathrm{d}R+\tfrac{1}{4}\pi\right)\right] \tag{11}$$

for the open channels $j = 1, 2, \ldots, n$, while for the closed channels

$$\psi_j^{(\alpha)}(R) = k_j^{-\frac{1}{2}}(R)\, A_{\alpha j} \sin \bar{\phi}_j(R) \tag{12}$$

as required by the JWKB boundary conditions at an outer turning point b_j. Equations (11) and (12) require that

$$\sum_l B_{\alpha l}(1+\mathrm{e}^{2\mathrm{i}\delta_l})\, T_{lj} = \begin{cases} \delta_{\alpha j}, & j = 1, \ldots, n, \\ 0, & j = n+1, \ldots, N, \end{cases} \tag{13}$$

and

$$\sum_l B_{\alpha l}(1-\mathrm{e}^{2\mathrm{i}\delta_l})\, T_{lj} = -\mathrm{i}K_{\alpha j}, \quad j = 1, \ldots, n. \tag{14}$$

The orthogonality of the matrix T ensures that equations (13) are satisfied by the choice,

$$B_{\alpha l} = \tilde{T}_{\alpha l}(1+\mathrm{e}^{2\mathrm{i}\delta_l})^{-1}, \quad \alpha = 1, \ldots, n, \tag{15}$$

which means, if the subscript j is replaced by β for notational symmetry, that

$$\begin{aligned} K_{\alpha j} = K_{\alpha\beta} &= \mathrm{i}\sum_l \tilde{T}_{\alpha l}(1+\mathrm{e}^{2\mathrm{i}\delta_l})^{-1}(1-\mathrm{e}^{2\mathrm{i}\delta_l})\, T_{l\beta} \\ &= -\sum_l \tilde{T}_{\alpha l} \tan\delta_l\, T_{l\beta}. \end{aligned} \tag{16}$$

Finally, the physical $n \times n$ scattering matrix may be expressed (Child 1974),

$$S = (I - \mathrm{i}K)^{-1}(I + \mathrm{i}K), \tag{17}$$

with the K matrix elements given by equation (16).

In the context of unimolecular dissociation, the next step is to analyse S (or K) for resonance behaviour by looking for abrupt changes in the eigenphase sum $\Sigma_i \eta_i$ as the energy increases, where the η_i are obtained by diagonalizing S and K in the forms

$$S = \tilde{X}\, \mathrm{e}^{2\mathrm{i}\eta} X, \quad K = \tilde{X} \tan \eta X. \tag{18}$$

The rate of dissociation is then obtained in the normal way (Child 1974) from the energy derivative of the η_i, while the populations in the different channels are determined by the elements $|X_{i\alpha}|^2, \alpha = 1, \ldots, n$.

3. Isolated resonance approximation

The simplest case occurs when the resonance is isolated in the sense that the abrupt change in the eigenphase sum is attributable to a single term. Comparison between equations (16) and (18) shows that this behaviour will occur around energies at which $\delta_k = (n_k + \frac{1}{2})\pi$ because the kth term will dominate on the right-hand side of equation (16) giving rise to the factorization,

$$K = \tan\delta_k(\boldsymbol{t}_k\, \tilde{\boldsymbol{t}}_k), \tag{19}$$

where $\boldsymbol{t}_k$ and $\tilde{\boldsymbol{t}}_k$ are the column and row vectors with elements $\tilde{T}_{\alpha k}$ and $T_{k\alpha}$ respectively ($\alpha = 1, 2, \ldots, n$). A matrix of this form is readily verified to have a single non-zero eigenvalue, given by

$$\tan\eta_k = \tan(\delta_k)\, \tilde{t}_k t_k = \tan\delta_k \sum_{\alpha=1}^{n} |T_{k\alpha}|^2, \tag{20}$$

corresponding to the normalized eigenvector

$$X_k = \boldsymbol{t}_k(\tilde{\boldsymbol{t}}_k\, \boldsymbol{t}_k)^{-\frac{1}{2}}. \tag{21}$$

The remaining eigenvectors $\boldsymbol{u}$ are necessarily orthogonal to $\boldsymbol{t}_k$ (i.e. $\tilde{\boldsymbol{t}}_k \boldsymbol{u} = 0$) because K is symmetric; hence

$$K\boldsymbol{u} = \tan(\delta_k)\, \boldsymbol{t}_k \tilde{\boldsymbol{t}}_k \boldsymbol{u} = 0, \tag{22}$$

which confirms that the remaining eigenvalues are all zero.

The conclusion is that the resonance behaviour is concentrated in the term

$$\eta_k = \arctan(\epsilon_k \tan \delta_k), \tag{23}$$

where

$$\epsilon_k = \tilde{\boldsymbol{t}}_k \boldsymbol{t}_k = \sum_{\alpha=1}^{n} |T_{k\alpha}|^2. \tag{24}$$

Hence, to the extent that changes in ϵ_k may be ignored around the resonance point, the collision delay time may be estimated as

$$\tau_k(E) = \frac{2\,\mathrm{d}\eta_k}{\mathrm{d}E} = \frac{2\epsilon\hbar \sec^2 \delta_k}{1+\epsilon^2 \tan^2 \delta_k}\left(\frac{\mathrm{d}\delta_k}{\mathrm{d}E}\right). \tag{25}$$

Equation (24) may be simplified by means of the approximation

$$\delta_k \approx (n+\tfrac{1}{2})\,\pi + (E - E_k)\,\pi/\hbar\tilde{\omega}_k, \tag{26}$$

where $\hbar\tilde{\omega}_k$ is the energy separation between resonances in the eigenchannel. One finds after some manipulation that for energies close to E_k

$$\tau_k(E) = \frac{\hbar\Gamma_k}{(E-E_k)^2 + \frac{1}{4}\Gamma_k^2}, \tag{27}$$

with the resonance width Γ_k given by

$$\Gamma_k = 2\epsilon_k \hbar\tilde{\omega}_k/\pi. \tag{28}$$

The delay time on resonance ($E = E_k$) is therefore

$$\tau_k(E_k) = 4\hbar/\Gamma_k = 2\pi/\epsilon_k \tilde{\omega}_k. \tag{29}$$

Alternatively the state specific rate constant, which may be identified with the inverse of half the collision delay time, may be expressed as

$$k_k = 2[\tau_k(E_k)]^{-1} = \epsilon_k \tilde{\omega}_k/\pi. \tag{30}$$

Finally, the populations in different fragmentation channels are given by

$$P_\alpha = |X_{\alpha k}|^2 = |T_{\alpha k}|^2 \Big/ \sum_{l=1}^{n} |T_{\alpha l}|^2. \tag{31}$$

Equations (28)–(31) are central results of the theory.

To see their physical significance, notice that the factor $(2\pi/\tilde{\omega}_k)$ in equation (29) may be interpreted as the time period for oscillatory internal radial motion in the kth eigenchannel. Consequently $(\tilde{\omega}_k/\pi)$ in equation (30) is the rate at which complexes emerge from the internal region to approach the transition state, while ϵ_k gives the probability of crossing into the fragmentation region. (Equation (23) shows that $\epsilon_k \leqslant 1$ because the orthogonality of T ensures that

$$\sum_{\alpha=1}^{N} |T_{\alpha k}|^2 = 1,$$

where N is the total number of coupled internal channels.) The fragmentation channel populations are then determined by the open channel components of the kth eigenvector $\boldsymbol{t}_k$ of Σ.

This structure encompasses a range of possibilities. At one extreme Σ may be assumed to be near diagonal, in which case the diagonal elements of T are close to unity and the off-diagonal elements are small. Physically this means that some of the eigenchannels are almost completely open with $\epsilon_k \approx 1$ in equations (28)–(30), and others almost completely closed with $\epsilon_k \ll 1$; different resonances therefore have widely different lifetimes. The opposite limit is a statistical one in which

$$|T_{\alpha k}|^2 \approx 1/N, \tag{32}$$

for all α and k, so that according to equation (24)

$$\epsilon_k \approx \epsilon_{\text{stat}} \approx (n/N). \tag{33}$$

Equation (30) then has an RRKM-like interpretation (Robinson & Holbrook 1972; Forst 1973) in the sense that the decomposition rate depends on a factor $(\tilde{\omega}_k/\pi)$, which represents the rate of arrival at the transition state multiplied by the fractional number of open channels in the total coupled by the matrix Σ.

4. Model application

The theory was applied to a simplified model for the in plane dissociation of HCN based on the hamiltonian

$$H = -\frac{\hbar^2}{2m}\frac{\partial^2}{\partial R^2} - \frac{\hbar^2}{2mR^2}\frac{\partial^2}{\partial \theta_R^2} - \frac{\hbar^2}{2\mu r_e^2}\frac{\partial^2}{\partial \theta_r^2} + W(R, r_e, \chi), \tag{34}$$

where $\chi = \theta_R - \theta_r$,

$$W(R, r_e, \chi) = D + A(\chi)\,\mathrm{e}^{-2\beta(R-R_e)} - 2D\,\mathrm{e}^{-\beta(R-R_e)}, \tag{35}$$

$$A(\chi) = A_0 + A_1 \cos\chi + A_2 \cos 2\chi, \tag{36}$$

and m and μ are the reduced masses of H with respect to CN and of the diatomic CN respectively. The parameter values $D = 5.65$ eV, $A_0 = 7.5025$ eV, $A_1 = -0.265$ eV, $A_2 = -1.5875$ eV, $\beta = 1.860$ Å, $R_e = 1.686$ Å and $r_e = 1.17$ Å were chosen for consistency with the dissociation energies of HCN and HNC (5.65 eV and 5.164 eV respectively (Herzberg 1976; Maki & Sams 1981)), an isomerization saddle point energy of 2.1 eV (Pearson *et al.* 1978), $\nu_{\text{CH}} = 3311$ cm^{-1} and the geometry of HCN (Herzberg 1976). Note that motions of the CN vibration have been suppressed and that the potential anisotropy is probably unduly concentrated in the repulsive term in equation (36) compared with the form suggested by Murrell *et al.* (1984).

The reference potentials used in equation (2) were taken as

$$V_j(R) = \frac{j^2\hbar^2}{2mR^2} + \frac{l^2\hbar^2}{2\mu r_e^2} + W_0(R, r_e), \tag{37}$$

where $W_0(R, r_e)$ includes only the isotropic term in equation (36) and l and j are related by the total angular momentum constraint $l + j = J$. The internal S matrix elements were then approximated in the discretized sudden form

$$\underset{jj'}{\Sigma} = \sum_i \psi_j^*(\chi_i)\,\mathrm{e}^{2\mathrm{i}\eta(\chi_i)}\psi_{j'}(\chi_i), \tag{38}$$

where

$$\eta(\chi_i) = \int_{a_i}^{R_c} k(R, \chi_i)\,\mathrm{d}R - \int_{a_0}^{R_c} k_0(R)\,\mathrm{d}R$$

$$\psi_j(\chi_i) = (2\pi)^{-\frac{1}{2}}\mathrm{e}^{\mathrm{i}j\chi_i}. \tag{39}$$

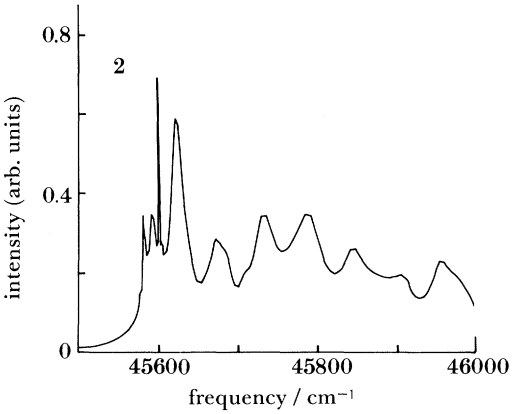

Figure 2. A crudely simulated absorption spectrum, with intensity governed by the Franck–Condon overlap with the ground bending state as in equations (40) and (41).

The number of χ_i values (which were chosen to be equally spaced between 0 and 2π) was taken equal to the number of channels to be included, and Σ was factored into even and odd blocks by transformation to real trigonometric basis functions, in the usual way. It was found that 60 channels were required for convergence, and that the matrix Σ was sufficient slowly varying to allow interpolation for its elements over a grid with energy spacings of 50 cm^{-1}.

Preliminary results are presented in figures 2 and 3, within the isolated resonance approximation. The resonance energies were obtained by interpolation for the points at which $\delta_k = (n_k + \frac{1}{2})\pi$ in one or other of the eigenchannels, these being ordered according to their eigenvector overlap with those at a central energy point in the interpolation grid. The resonance widths were given by equation (28). The typical computation time was 15 min CPU on a VAX 8600 series computer to characterize 100 resonances over a 400 cm^{-1} wavenumber interval.

Figure 2 shows a simulated absorption excitation spectrum for the production of CN radicals, with a Franck–Condon like measure of intensity,

$$\langle \psi_0 | \psi_k \rangle = \sum_j a_j T_{kj}, \tag{40}$$

where T_{kj} are the components of the resonance eigenvector and a_j are the components of an angular momentum decomposition of the ground bending vibrational state

$$a_j = (\pi)^{-\frac{1}{2}} \int_0^\pi \psi_0(\chi) \cos(j\chi)\, \mathrm{d}\chi \approx \left(\frac{4}{\beta\pi}\right)^{\frac{1}{4}} \mathrm{e}^{-j^2/2\beta}, \tag{41}$$

with $\beta^2 = \hbar/(I^* k_{\chi\chi})^{\frac{1}{2}}$ and $I^* = \mu r_e^2\, mR_e^2/(\mu r_e^2 + mR_e^2)$. The peaks in figure 2 therefore correspond to upper state eigenchannels with the highest zero-point bending character, but it should be noted that the motions in this energy region resemble internal rotation rather than bending and that $|\langle \psi_0 | \psi_k \rangle|^2 \leqslant 0.15$ even for the strongest peaks.

Further information is provided in figure 3, which shows the individual resonance positions and widths, together with the fragment populations in the ten lowest channels. The scale of Γ shows that each peak in figure 2 covers many resonances. One also sees, as expected that the resonance widths, which determine the decay

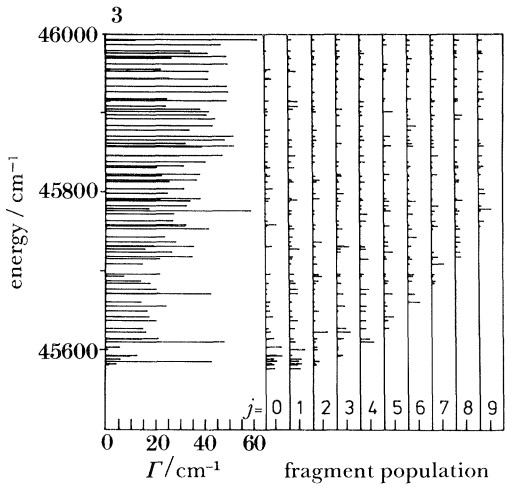

Figure 3. Energy variation of the isolated resonance widths (left-hand panel) and fragment channel populations (right-hand panel) over the energy range of figure 2.

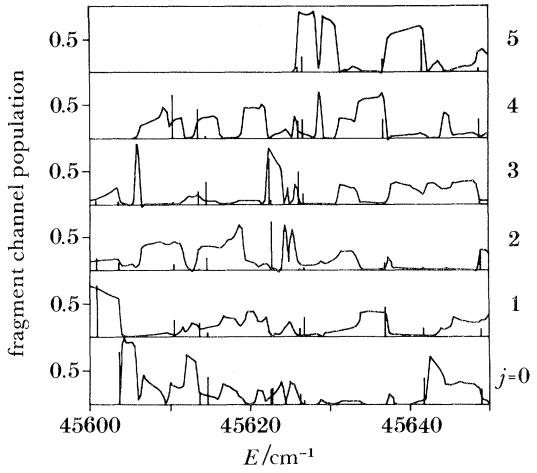

Figure 4. Energy variation of the fragment channel populations associated with the closest resonance after taking account of inter-resonance coupling. Vertical lines indicate isolated resonance positions and fragment populations. The energy range covers the main peak in figure 2.

rate, broadly increases as the number of open channels increases with increasing energy. Moreover, apart from a few very sharp levels, close to threshold, the widths in any given energy region differ at most by a factor of order two, which implies a more or less statistically determined decomposition rate. Such a statistical picture is, however, less well supported by the fragment state populations, which show marked preferences for particular channels that vary from resonance to resonance.

The fact that the typical resonance width greatly exceeds the spacing from one resonance to the next clearly casts doubt on the isolated resonance approximation. Hence a full investigation of the effects of overlapping resonances was done, by analysis of the eigenvectors of the physical S matrix, given by equations (16)–(18). Results are illustrated in figure 4 for the fragment state populations determined by the eigenvector of S with the largest value of $\tan\eta$ (i.e. for the eigenchannel of S

closest to resonance). In the isolated resonance approximation such a plot would yield a series of steps, with heights determined by the sticks in figure 4. The calculated picture is more complicated because, although many of the population changes occur around the isolated resonance positions there are a number of features, such as the peaks in the $j = 3$ and $j = 4$ populations at 45606 cm^{-1} and 45629 cm^{-1} respectively, that can only be attributed to quantum mechanical interference.

5. Summary and conclusions

The techniques of generalized multichannel quantum defect theory have, for the first time, been used to formulate a unified quantum mechanical theory of bound states and unimolecular dissociation. The central quantity is an internal scattering matrix $\tilde{\Sigma}$, whose eigenchannels support the bound states and the projection of whose eigenvectors onto the physically open channels determines both the decay rates and the fragment state populations. A 'statistical eigenvector', isolated resonance version of the theory bears a close similarity to currently accepted statistical unimolecular dissociation models, but the full formulation makes no statistical assumptions.

Preliminary results from a 60 channel model study of the in-plane dissociation of HCN were reported, with $\tilde{\Sigma}$ determined by the sudden approximation. It was found that the distribution of decay rates, over different resonances, was broadly statistical, being largely governed by the fraction of open channels. The distribution over fragment states, from any given resonance, was much less statistical in character, with many specific preferences for particular channels. Gross features of the fragment state distributions were moderately insensitive to interactions between the many overlapping isolated resonances, but some variations could only be attributed to quantum mechanical interference.

The author is grateful to Dr F. H. Mies for comments on an early draft of the paper.

References

Aquilanti, V. & Cavalli, S. 1987 *Chem. Phys. Lett.* **133**, 538.
Butler, L. J., Tichich, T. M., Likar, M. D. & Crim, F. F. 1986 *J. chem. Phys.* **85**, 2331.
Burke, P. G. 1968 *Adv. Atom. Molec. Phys.* **4**, 173.
Carrington, A. & Kennedy, R. A. 1984 *J. chem. Phys.* **81**, 91.
Child, M. S. 1974 *Molecular collision theory.* New York: Academic Press.
Child, M. S. 1986 *J. phys. Chem.* **90**, 3595.
Fano, U. 1970 *Phys. Rev.* A **2**, 353.
Forst, W. 1973 *Theory of unimolecular reactions.* New York: Academic Press.
Greene, C. H. & Jungen, Ch. 1985 *Adv. atom. molec. Phys.* **21**, 51.
Guyer, D. R., Polik, W. F. & Moore, C. B. 1984 *J. chem. Phys.* **84**, 91.
Herzberg, G. 1976 *Electronic spectra of polyatomic molecules.* van Nostrand.
Holmer, B. K. & Child, M. S. 1983 *Faraday Discuss. chem. Soc.* **75**, 131.
Maki, A. G. & Sams, R. L. 1981 *J. chem. Phys.* **75**, 4178.
Mies, F. H. & Krauss, M. 1966 *J. chem. Phys.* **45**, 4455.
Mies, F. H. 1969 *J. chem. Phys.* **51**, 787, 798.
Mies, F. H. & Julienne, P. 1984 *J. chem. Phys.* **80**, 2514, 2526.
Murrell, J. N., Carter, S., Farantos, S. C., Huxley, P. & Varandas, A. J. C. 1984 *Molecular potential energy functions.* New York: Wiley.

PHILOSOPHICAL TRANSACTIONS OF THE ROYAL SOCIETY A MATHEMATICAL, PHYSICAL & ENGINEERING SCIENCES

Pearson, P. K., Schaefer, H. F. & Wahlgren, U. 1975 *J. chem. Phys.* **62**, 350.
Reisler, H. & Wittig, C. 1986 *A. Rev. phys. Chem.* **37**, 307.
Robinson, J. P. & Holbrook, K. A. 1972 *Unimolecular reactions*. New York: Wiley.
Seaton, M. J. 1983 *Rep. Prog. Phys.* **46**, 167.
Waite, W. A. & Miller, W. H. 1980 *J. chem. Phys.* **73**, 3713.
Waite, W. A. & Miller, W. H. 1981 *J. chem. Phys.* **74**, 3910.

Discussion

J. C. Light (*University of Chicago, U.S.A.*). It is, also, quite straightforward to obtain both bound and resonance states in a unified fashion from a single L^2 calculation. In this case the eigenvectors correspond to both bound states and to (approximate) resonance and scattering states embedded in the continuum. The resonance states may be identified using multiple L^2 calculations and stability analysis or from a single L^2 calculation by evaluating the expectation value of an outgoing flux operator (Choi & Light 1990). The resonance energies are obtained with accuracy comparable with those of the bound states.

N. C. Handy (*University of Cambridge, U.K.*). I support the comments of Professor Light, that the use of basis sets presents a unified picture for bound and continuum states. An elementary example concerns the polarizability of the H atom. Using second-order perturbation theory, it may be shown that bound np_z H states predict a polarizability of 3.645 a.u.† and that continuum p_z states contribute the extra 0.855 a.u. to give the exact value of 4.5 a.u. On the other hand, a calculation of the polarizability by the finite field approach, using a basis set of the form $z\,\mathrm{e}^{-\alpha r}$, rapidly converges to the exact value.

M. S. Child. In answer to the comments by Dr Handy and Professor Light, the use of basis sets may well be the way forward, particularly in view of the computational efficiency of the discrete variable representation.

The eigenchannel version of generalized quantum defect theory that I described has, however, certain advantages. The necessary internal S matrices and phase terms are all smooth functions of energy; hence sharp resonance features can be reproduced even by interpolation over a coarse energy grid. Secondly, the eigenchannels unify the bound and resonant states in a manner similar to that of the Wigner R matrix method, but the scattering formulation reduces the size of the matrices to be handled by a factor equal to the number of states in a channel.

Additional reference

Choi, S. & Light, J. C. 1990 *J. chem. Phys.* **92**, 2129.

† 1 a.u. $= 1.648 \times 10^{-41}\ \mathrm{J^{-1}\ C^2\ m^2}$.